Plasmid DNA Adsorption on Silica: Kinetics and Conformational Changes in Monovalent and Divalent Salts

Thanh H. Nguyen*,† and Menachem Elimelech‡

Department of Civil and Environmental Engineering, University of Illinois at Urbana-Champaign, Urbana, Illinois 61801, and Department of Chemical Engineering, Environmental Engineering Program, Yale University, New Haven, Connecticut 06520-8286

Received April 23, 2006; Revised Manuscript Received July 27, 2006

A quartz crystal microbalance with dissipation (QCM-D) is used to determine the adsorption rate of a supercoiled plasmid DNA onto a quartz surface and the structure of the resulting adsorbed DNA layer. To better understand the DNA adsorption mechanisms and the adsorbed layer physicochemical properties, the QCM-D data are complemented by dynamic light scattering measurements of diffusion coefficients of the DNA molecules as a function of solution ionic composition. The data from simultaneous monitoring of variations in frequency and dissipation energy with the QCM-D suggest that the adsorbed DNA layer is more rigid in the presence of divalent (calcium) cations compared to monovalent (sodium) cations. Adsorption rates are significantly higher in the presence of calcium, attaining a transport-limited rate at about 1 mM Ca^{2+}. Results further suggest that in low ionic strength solutions containing 1 mM Ca^{2+} and in moderately high ionic strength solutions containing 300 mM NaCl, plasmid DNA adsorption to negatively charged mineral surfaces is irreversible.

Introduction

Adsorption of biological macromolecules to solid surfaces has important applications in DNA microarrays,[1,2] gene therapy,[3,4] DNA-based sensors,[5−7] high-quality DNA purification by chromatographic techniques,[8] DNA hybridization studies,[9,10] and the development of platforms for studying protein−DNA interactions.[11] For a number of microorganisms, the initial stage of biofilm formation is facilitated by the attachment of extracellular DNA on the substrate surface.[12] A thorough understanding of DNA adsorption to surfaces is therefore necessary to control the formation of bacterial biofilms. In addition, adsorption of extracellular DNA to mineral surfaces in subsurface environments has been shown to provide physical protection for the DNA from enzymatic degradation.[13,14] More importantly, the adsorbed DNA retains its ability to transform competent microorganisms via horizontal gene transfer, thus giving rise to microbial diversity.[13,15,16]

Several studies have addressed the adsorption mechanisms of DNA molecules to negatively charged mineral surfaces. Romanowski et al.[13] used flow-through columns to show significant adsorption of 2.4 kb plasmid DNA to natural sands in the presence of at least 100 mM NaCl or of more than 1 mM $MgCl_2$. It was suggested that charge neutralization of the DNA phosphate backbones and the silica surfaces by cations controls DNA adsorption. Cation bridging between the DNA molecules and mineral surfaces has also been suggested to explain adsorption to quartz sand[14] or to clay minerals.[17] Recently Libera et al.[18] used X-ray standing waves to study adsorption of synthetic RNA molecules (mercurated polyuridilic acid) to a silica surface in the presence of Zn^{2+}. In contrast to previous studies,[13,14,17] Libera et al.[18] proposed that the formation of $SiOZn^{+}$ groups at the silica surface promotes adsorption of the RNA molecules. Adsorption of DNA molecules to mica surfaces has been studied extensively by atomic force microscopy (AFM).[19,20] Enhancement in DNA immobilization to mica surfaces in divalent cation solutions has been observed. This behavior has been explained by different mechanisms, including charge neutralization of the DNA phosphate backbones[19] and the ability of cations to fit into microcavities on the mica surface.[20]

Debate on the adsorption mechanisms of DNA to negatively charged surfaces is based primarily on experimental data obtained from batch systems at equilibrium. The kinetics of DNA adsorption to negatively charged surfaces and the detachment of adsorbed DNA from surfaces as a function of solution chemistry have not been addressed in previous studies. Real time investigations on the conformational changes of adsorbed DNA layers have been attempted using AFM.[21,22] AFM images, however, are prone to artifacts and can only reveal the DNA conformation from above. No quantitative information on the structural properties of the DNA adsorbed layer can be obtained from AFM imaging.

This study aims at filling this gap by measuring adsorption kinetics, adsorption reversibility, and the changes in viscoelastic properties of the adsorbed DNA layer onto silica surfaces at different solution ionic compositions. We employed an ultrasensitive device, a quartz crystal microbalance with dissipation (QCM-D), to simultaneously monitor the variations of adsorbed layer thickness and viscoelastic properties as a function of aqueous solution chemistry. Adsorption mechanisms and conformational changes of the adsorbed layer were revealed by analyzing the QCM-D data in conjunction with diffusion coefficients measured by dynamic light scattering (DLS) at various ionic compositions.

Materials and Methods

Plasmid DNA Preparation and Characterization. Plasmid vector pGEM-Teasy (3015 bp) was electroporated into *E. coli* XL1 blue. For

* To whom correspondence should be addressed. Phone: 217-244-5965. Fax: 217-333-6968. E-mail: thn@uiuc.edu.
† University of Illinois at Urbana-Champaign.
‡ Yale University.

10.1021/bm0603948 CCC: $37.00
Published on Web 12/15/2006

plasmid DNA extraction and purification, we grew 5 L of this *E. coli* strain in LB broth containing 0.1 mg/mL ampicillin for approximately 12 h. The cell density was approximately 10^9/mL as measured by a UV spectrophotometer (SmartSpect 3000, Bio-Rad Labratories, CA). The plasmid DNA extraction was performed using Qiagen EndoFree Plasmid Giga kits according to the protocol recommended by the company (Qiagen Inc. CA). The extracted plasmid DNA was dissolved in 20 mL of deionized (DI) water. To facilitate dissolution of the extracted DNA, the DI water was adjusted to pH 8.0 by adding 1 M NaOH. The deionized water was purchased from American Bioanalytical (Natick, MA) and was tested for RNase and endotoxins by the company. The plasmid DNA solution was then divided into 0.2 mL aliquots and kept in microcentrifuge tubes at −20 °C until use. The concentration of plasmid DNA stock solution was 1700 mg/L as measured by a UV spectrophotometer. For this measurement, a calibration curve was generated using diluted standard solutions of salmon sperm DNA at 10 mg/mL (Invitrogen). A 5 μL portion of the plasmid DNA solution diluted 100 times was used for agarose gel electrophoresis. A 1% agarose gel was prepared and stained with ethidium bromide after 1 h of electrophoresis at 100 V. A supercoiled plasmid ladder (Invitrogen) was also used to check the integrity of the extracted plasmid.

Solution Chemistries. Solutions for QCM-D experiments were prepared with DI water and filtered through a 0.22 μm filter (Whatman, Middlesex, UK). Two sets of solutions were prepared: solutions at pH 5.9 ± 0.1 (referred to as pH 6) and solutions at pH 7.9 ± 0.1 (referred to as pH 8) buffered by 1 mM $NaHCO_3$. For solutions containing $CaCl_2$ (from 0.1 to 1.0 mM), NaCl was added to maintain a total ionic strength of 10 mM. Solutions were prepared before the QCM-D experiments and were kept at 4 °C until use. Analytical grade chemical compounds, including NaCl, $CaCl_2$, $MgCl_2$, $NaHCO_3$, poly-L-lysine hydrobromide, and the HEPES buffer were purchased from Sigma.

Determination of Plasmid Diffusion Coefficients by Dynamic Light Scattering (DLS). The plasmid DNA diffusion coefficients were measured in various solution chemistries using a multidetector light-scattering unit (ALV-5000, Langen, Germany). The light source was a solid-state, diode-pumped, frequency-doubled, Nd:vanadate (Nd:YVO_4) laser (Verdi 2, Coherent, Santa Clara, CA) operating at a wavelength of 532 nm. Eight optical fiber photodetectors were mounted on a compact goniometer system. The sample vials were placed in a thermostated index-matching quartz vat filled with toluene and double-filtered with a 0.1 μm filter (Puradisk 25 TF, Whatman, Middlesex, UK).

Disposable glass sample vials and their Teflon-lined caps were purchased from Supecol (Bellefonte, PA). Before use, the glass vials and their caps were soaked in 2% Extran MA01 solutions (Merck, KgaA, Darmstadt, Germany) overnight, thoroughly rinsed with deionized water, and oven-dried at 60 °C under dust-free conditions. Immediately before the measurements, aliquots of plasmid DNA solutions were warmed up to room temperature (23 °C). For each measurement, 1.9 mL of the electrolyte solution and 0.2 mL of the plasmid DNA stock solution were gently mixed in a 15-mL plastic centrifuge tube. Next, 2.0 mL of the electrolyte and plasmid DNA mixture was slowly transferred into the glass sample vials, which were then closed with Teflon-lined caps for DLS measurements. The concentration of the plasmid DNA for the DLS measurements was 160 mg/L.

All light scattering measurements were conducted by positioning the detector at a scattering angle of 90° from the incident laser beam. The detector signal was fed into the correlator, which accumulated each autocorrelation function for 15 s. A second-order cumulant fit was used to analyze the autocorrelation functions and to determine the intensity-weighted diffusion coefficients. For each sample, 40 autocorrelation functions were obtained during the 600-s measurement.

Quartz Crystal Microbalance with Dissipation (QCM-D). The QCM-D measurements were performed with AT-cut quartz crystals mounted in a D300 system (Q-sense AB, Gothenburg, Sweden). The crystals, with a fundamental resonant frequency $f_0 \approx 5$ MHz, were coated with amorphous silica by vapor deposition and were supplied by Q-sense (batch 051031). Before each measurement, the crystals were soaked in a 2% Hellmanex II solution (Hellma GmbH & Co KG, Müllheim, Germany) overnight, rinsed thoroughly with deionized water, dried with ultrahigh-purity N_2 gas, and treated for 25 min in a UV/O_3 chamber.

For these experiments, the variations of frequency (Δf) and dissipation factor (ΔD) were measured for three overtones ($n = 3$, 5, and 7). The interpretation of the viscoelastic properties of the adsorbed layers was based on the Voigt model, as presented in Voinova et al.[23] The solution density and viscosity used in this model were 1000 kg/m^3 and 10^{-3} Pa s, respectively. The density of the adsorbed layer was fixed at 1030 kg/m^3, following the recommendations of Gurdak et al.[24] The best fitting values for shear viscosity (η), shear modulus (μ), and Voigt thickness (d_{Voigt}) of the adsorbed layer were obtained by modeling the experimental data of Δf and ΔD for at least two overtones using the program Q-Tools provided by Q-Sense AB. This program applies a curve-fitting algorithm that searches for the unknown parameters (η, μ, d_{Voigt}) by minimizing the χ^2 parameter. Modeling was performed using the same initial parameters for four combinations of experimental data collected at different overtones (i.e., $n = 3$, 5; 3, 7; 5, 7; and 3, 5, 7). The fitting results were qualitatively similar for all cases, indicating that the viscoelastic properties were frequency independent. Fitted parameters were forced between maximal and minimal guesses for viscosity (10^{-5}, 10^{-2} Pa s), shear modulus (10^3, 3×10^6 Pa), and Voigt thickness of the adsorbed layer (0.1, 20 nm). A similar modeling approach for an adsorbed DNA layer was applied successfully by Stengel et al.[25]

Protocol for Plasmid Adsorption Kinetics Studies. All QCM-D experiments were performed under flow-through conditions using a syringe pump (Kd Scientific Inc. Holliston, MA) operating in suction mode. Specifically, the pump was connected to the sensor crystal outlet, and the studied solutions, contained within a syringe connected to the sensor crystal inlet, were fed through the crystal sensor chamber at 0.1 mL/min. Electrolyte solutions for the QCM-D experiments were degassed by sonicating for at least 20 min and subsequently kept at 27 °C until being introduced into the QCM-D system. The aliquots of plasmid DNA solutions, kept at −20 °C, were taken out of the freezer immediately before use and allowed to warm up to room temperature. Before the adsorption experiments, 0.2 mL of plasmid DNA stock solution was added to 1.8 mL of an appropriate electrolyte solution to obtain a 2 mL electrolyte solution containing 170 mg/L plasmid DNA. For all experiments, the QCM-D system was equilibrated with the corresponding electrolyte solution for a minimum of 30 min to establish a stable baseline before the addition of the plasmid DNA electrolyte solution. For adsorption kinetics experiments, data were collected for approximately 20 min after the introduction of plasmid DNA solution to the QCM-D system. The adsorption rate was taken as the initial slope of the normalized frequency shift at the third overtone ($\Delta f_{(3)}$) vs time curve.

For experiments that examined the reversibility and structural changes of the plasmid DNA adsorbed layer, 2-mL solutions were added sequentially to the QCM-D system in the following order: (1) plasmid DNA in divalent cation salt solution, (2) the same electrolyte solution without plasmid DNA, (3) monovalent salt solution of 10 mM ionic strength, and (4) monovalent salt solution of 1 mM ionic strength. The studied divalent salt solutions were 0.5, 0.7, and 1.0 mM $CaCl_2$ at pH 6 and pH 8 and 1.0 mM $MgCl_2$ at pH 6. For monovalent salt solutions of 10 mM ionic strength, 10 mM NaCl or 9 mM NaCl plus 1 mM $NaHCO_3$ solutions were used at pH 6 or pH 8, respectively. For the 1 mM monovalent salt solutions of 1 mM ionic strength, 1 mM NaCl or 1 mM $NaHCO_3$ solutions were used at pH 6 or pH 8, respectively. For experiments that investigated the conformational change of the plasmid DNA adsorbed layer in the presence of 300 mM NaCl, 2-mL solutions were added sequentially to the QCM-D system in the following order:

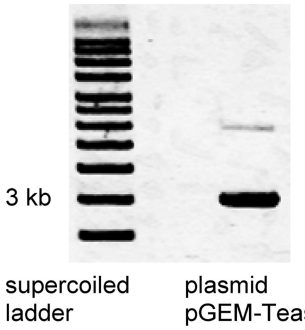

Figure 1. Agarose gel electrophoresis image of plasmid pGEM-Teasy. The major dark band, at 3 kb, shows the supercoiled form of the plasmid. The minor thin band, around 7.5 kb, shows the relaxed form of the plasmid.

(1) 0.4 mL of plasmid DNA stock solution in 1.6 mL of 300 mM NaCl solution, (2) 300 mM NaCl solution, (3) 30 mM NaCl solution, (4) 1 mM NaCl solution, and (5) deionized water. Each step lasted for approximately 20 min. Each set of experiments was performed at least twice to ensure experimental reproducibility.

Because silica has a point of zero charge near pH 3.0, the SiO_2 coating substrate is negatively charged at the studied pH (6.0 and 8.0). To obtain a positively charged surface for favorable adsorption, a layer of poly-L-lysine (PLL) was formed on the silica surface at pH 7.4. PLL was dissolved to a 0.1 g/L final concentration in a HEPES buffer (pH 7.4) made from 10 mM *N*-(2-hydroxyethyl)piperazine-*N*′-2-ethanesulfonic acid. After the QCM-D was equilibrated with the HEPES buffer, 2 mL of the PLL solution was added to the system and pumped through the crystal sensor chamber at 0.1 mL/min. The layer was washed with the HEPES buffer for 20 min and with 10 mM NaCl for another 20 min. After the two rinses, plasmid DNA solution in 10 mM NaCl was added to the system. The adsorption rate of plasmid DNA on the PLL layer was calculated as the initial slope of the frequency shift at the normalized third overtone ($\Delta f_{(3)}$) vs time when plasmid DNA adheres to the PLL layer. On the basis of three replicates, the plasmid DNA adsorption rate on the PLL layer was 15.79 ± 1.25 Hz/min. Attachment efficiency, α, was then calculated as the measured adsorption rate at a given experimental condition normalized by the adsorption rate on the PLL layer.

Results and Discussion

Plasmid DNA Preparation and Characterization. The A_{260}/A_{280} ratio for the plasmid DNA solution was 2.0, indicating that the plasmid DNA solution was not contaminated by proteins.[26,27] Two bands were observed in the agarose gel (Figure 1): a broadband at 3 kb and a much smaller band at around 7.5 kb. Thus, we conclude that the vast majority of the extracted plasmid is in the supercoiled form.

Influence of Ionic Composition on Plasmid Diffusion Coefficients. Figure 2 presents the average and standard deviation of plasmid DNA diffusion coefficients measured by DLS in NaCl and $CaCl_2$ solutions. For each sample, 40 autocorrelation functions were obtained, with each measurement taking place for 600 s. During this 600-s measurement, we did not observe any systematic change in diffusion coefficients as a function of time. The R^2 values for a linear correlation between diffusion coefficients and time were less than 0.1. This observation indicates that plasmid DNA molecules were stable and did not aggregate under the studied conditions.

As shown in Figure 2, at both pH 6 and 8, diffusion coefficients for the plasmid DNA are statistically higher in 10 mM than in 1 mM ionic strength solutions (one sided t test with 95% confidence). Observations of increased DNA diffusion

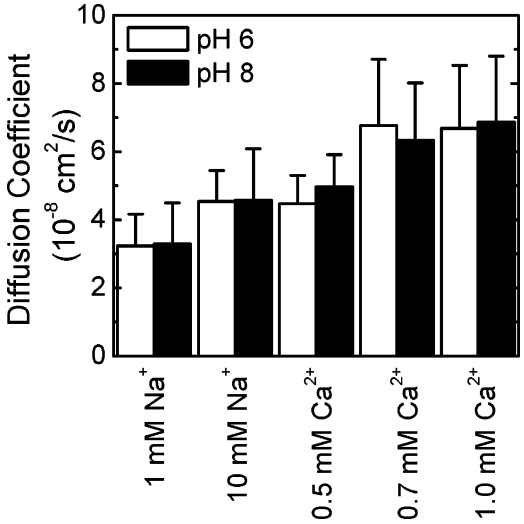

Figure 2. Diffusion coefficients of plasmid DNA in monovalent and divalent salt solutions at pH 6 and 8. $CaCl_2$ solutions have a total ionic strength of 10 mM, made by the specified calcium concentration plus NaCl. The presented data are averages and standard deviations for 40 measurements of a single sample. Plasmid DNA concentrations during the measurements were 160 mg/L. Measurements were carried out at a temperature of 23 °C.

coefficients with an increase in ionic strength were shown for linear plasmid DNA fragments of 2311 and 1500 bp in salt solutions with ionic strengths up to 10 mM.[28] The diffusion coefficients measured for our 3015 bp supercoiled plasmid are in the range of diffusion coefficients reported for similar plasmid at low salt concentration. For example, the diffusion coefficients measured in our study are 4.53×10^{-8} and 4.57×10^{-8} cm^2/s in 10 mM Na^+ at pH 6 and 8, respectively. Reported diffusion coefficients are 4.67×10^{-8} cm^2/s for a 2311 bp relaxed circular plasmid in 10 mM CsCl[29] and 4.37×10^{-8} cm^2/s for a 2311 bp linear plasmid in 7 mM NaCl.[28]

For Ca^{2+}-containing solutions at 10 mM total ionic strength, the plasmid DNA diffusion coefficient increases with increasing $CaCl_2$ concentration. This observation suggests that the increase in Ca^{2+} concentration in solution leads to smaller plasmid DNA molecules. Even though the diffusion coefficient for plasmid DNA in 0.5 mM Ca^{2+} solution is approximately the same as that in 10 mM Na^+, the diffusion coefficients with 0.7 and 1.0 mM Ca^{2+} are statistically higher than those in solutions without Ca^{2+} (one sided t test with 95% confidence). The presence of at least 0.7 mM Ca^{2+} clearly results in plasmid DNA molecules with more compact conformation and higher diffusion coefficients.

The plasmid DNA molecules are highly negatively charged at pH 6 and 8 due to their phosphate backbone. In high ionic strength solutions of NaCl, the intramolecular electrostatic repulsion among negatively charged subsections of the plasmid DNA is screened by the ions in solution. At low ionic strength, charge screening is much less effective, resulting in significant intramolecular electrostatic repulsion and, consequently, less compact plasmid DNA molecules with lower diffusion coefficients. Similar arguments on the dependence of DNA conformation on salt concentration were proposed elsewhere.[28,30,31] Previous studies have shown that Ca^{2+} forms complexes with the phosphate oxygen atoms of double-strand oligonucleotides.[32,33] The specific interaction of Ca^{2+} with the phosphate backbone significantly reduces the intramolecular electrostatic repulsion of the DNA molecules. In this case, the DNA molecules have a more compact conformation or smaller size,

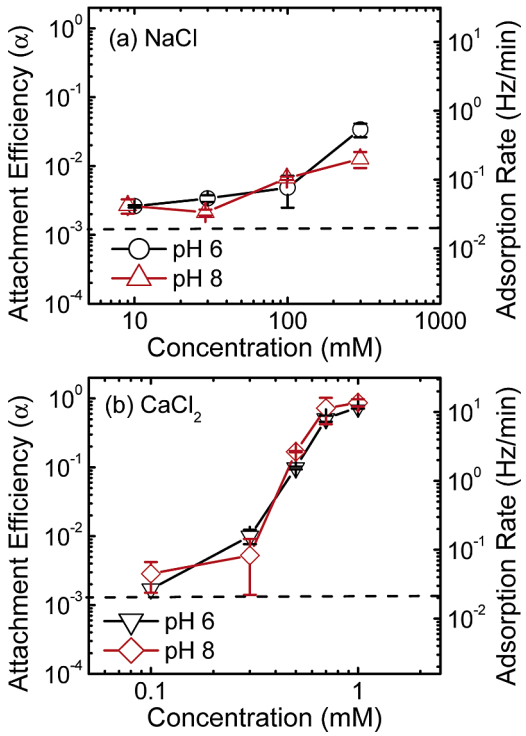

Figure 3. Adsorption kinetics of plasmid DNA onto silica surfaces at pH 6 and 8: (a) as a function of NaCl concentration and (b) as a function of $CaCl_2$ concentration (with the total ionic strength kept at 10 mM by proper addition of NaCl). Adsorption rates were taken as the initial slopes of the frequency shift curve at the normalized third overtone ($\Delta f_{(3)}$) vs time. Attachment efficiency is obtained by normalizing the actual plasmid adsorption rate by the adsorption rate on a PLL-coated silica surface layer (15.79 ± 1.25 Hz/min). Shown are average values of at least two replicate measurements. Error bars indicate standard deviations. Plasmid DNA concentrations during the experiments were 170 mg/L and the temperature was 25 °C. The horizontal dashed line at 0.02 Hz/min indicates the detection limit of the QCM-D measurement.

and therefore, their diffusion coefficients are higher than the case with an indifferent monovalent salt.

Kinetics of Plasmid DNA Adsorption. The plasmid adsorption rates and corresponding attachment efficiencies at pH 6 and 8 are presented in Figure 3. As described earlier, an attachment efficiency of 1.0 corresponds to favorable (nonrepulsive) adsorption conditions, when negatively charged plasmid DNA molecules adhere to a positively charged surface at a transport-limited rate. The plasmid adsorption kinetics behaviors are similar at the two pH conditions examined. In the absence of divalent cations (Figure 3a), the attachment efficiencies are low over the entire range of ionic strength studied. For 10 and 30 mM ionic strengths, the attachment efficiencies (0.003) are near the detection limit of the QCM-D measurement (shown by the horizontal dashed line). At 300 mM ionic strength, the attachment efficiency increases by about 1 order of magnitude to approximately 0.03 and 0.01 at pH 6 and 8, respectively. For 10 mM ionic strength, the presence of at least 0.5 mM calcium leads to a significant increase in the plasmid DNA adsorption rate and attachment efficiency (Figure 3b). For 1.0 mM $CaCl_2$, the attachment efficiencies are close to unity, averaging 0.75 ± 0.04 ($N = 4$) and 0.87 ± 0.10 ($N = 2$) at pH 6 and 8, respectively. In the 0.5 mM $CaCl_2$ solution, the attachment efficiencies for plasmid DNA adsorption are approximately 10 times higher than those in 300 mM NaCl. Thus, the presence of divalent cations leads to a substantial enhancement in plasmid adsorption compared to monovalent salts.

At the studied pH conditions, both the silica surface and plasmid DNA molecules are negatively charged. When the plasmid DNA molecules approach the silica surface, they encounter electrostatic repulsion, which is highly dependent on the solution chemistry. In the presence of monovalent cations (i.e., Na^+), the negative charges on the phosphate backbone of the plasmid DNA molecules are screened. This leads to an overall decrease in the electrostatic energy barrier between the silica surface and the DNA molecules and to an increase in adsorption rate, in qualitative agreement with the classic Derjaguin−Landau−Verwey−Overbeek (DLVO) theory. Stuart et al.[34] also showed that the attachment of polyelectrolytes to charged surfaces can be explained qualitatively by the DLVO theory. In another study, Romanowski[13] showed a 4-fold increased amount of plasmid DNA adsorption to quartz sand when the Na^+ concentration increased from 50 to 200 mM.

Divalent cations such as Ca^{2+} can chemically bind to the phosphate backbone, effectively neutralizing its negative charges. Consequently, the electrostatic repulsion between the DNA molecules and the silica surface is substantially reduced, resulting in a marked increase in adsorption rate. Ca^{2+} ions can also significantly reduce the charge of the silica surface by binding to silanol groups, which results in reduced electrostatic repulsion between the DNA and the silica surface.[18,35,36] Furthermore, in the presence of divalent cations, the DNA molecules have a more compact conformation and thus a higher diffusion coefficient due to the reduction in intramolecular electrostatic repulsion among subunits of the DNA molecules. The combination of DNA and silica charge neutralization by calcium ions, and, to a lesser extent, the concomitant increase in the DNA diffusion coefficient, lead to an increase in the adsorption rate of the plasmid DNA molecules on the silica surface. Similar enhancement in DNA adsorption to silica and mica surfaces by increasing ionic strength and divalent cations has been observed by several researchers.[13,14,21,37]

Structure of Adsorbed Plasmid DNA in Monovalent Salt. One of the advantages of the QCM-D is its ability to monitor the variations of the viscoelastic properties of the adsorbed layer, which are related to the conformation and structure of the adsorbed layer. A shortcoming of the QCM-D measurements, however, is that a clean crystal sensor may produce signals due to changes in electrolyte solutions flowing through the QCM-D system. For example, as shown in Figure 4a, a drop from 300 to 30 mM NaCl solution results in an increase of approximately 3 Hz for the frequency shift divided by the third harmonic number ($\Delta f_{(3)}$). This change in ionic strength also results in a decrease of the dissipation factor (D) by approximately 2×10^{-6}. Also, the frequency shift increases slightly and the dissipation factor decreases slightly, when we change the solution from 30 to 1 mM NaCl and from 1 mM NaCl to DI water. This effect is commonly referred to as the "buffer effect", because changes in viscosity and density of the solution lead to changes in frequency and dissipation measured by the QCM-D.[38,39]

Figure 4b depicts the variation in frequency and dissipation as a result of plasmid adsorption to silica when we used a solution containing 170 mg/L plasmid DNA in 300 mM NaCl. After the adsorption step (step 1) and a rinsing step with the same electrolyte solution of 300 mM (step 2), we rinsed the adsorbed layer with 30 mM NaCl (step 3). This change in ionic strength resulted in an increase in frequency of approximately

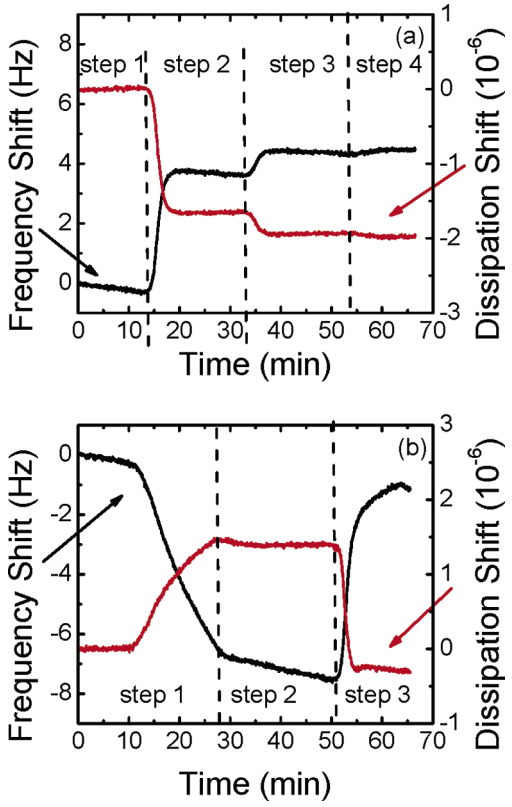

Figure 4. (a) Frequency shift divided by the third harmonic number ($\Delta f_{(3)}$) and associated dissipation shifts ($\Delta D_{(3)}$) as a function of time for different solutions at pH 6. Solution conditions were as follows: 300 mM NaCl (0−13 min, step 1), 30 mM NaCl solution (13−33 min, step 2), 1 mM NaCl (33−53 min, step 3), and DI water (step 4). (b) Frequency shift divided by the third harmonic number and associated dissipation shifts as a function of time for plasmid adsorption at pH 6. Plasmid concentration was 170 mg/L and the plasmid adsorption took place in 300 mM NaCl (step 1). The adsorbed plasmid layer was washed with 300 mM NaCl (30−50 min, step 2) and 30 mM NaCl solution (50−70 min, step 3).

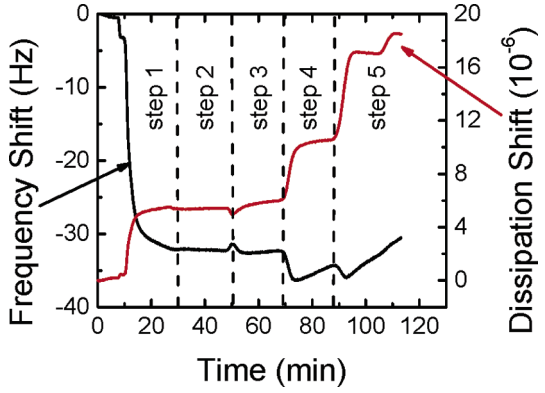

Figure 5. Frequency shift divided by the third harmonic number ($\Delta f_{(3)}$) and associated dissipation shifts ($\Delta D_{(3)}$) as a function of time for plasmid DNA adsorption at pH 6. Plasmid concentration in the adsorption experiments was fixed at 340 mg/L and the temperature was 25 °C. Plasmid adsorption occurred in 300 mM NaCl (step 1). The adsorbed plasmid layer was washed with 300 mM NaCl (30−50 min, step 2), 30 mM NaCl solution (50−70 min, step 3), 1 mM NaCl solution (70−90 min, step 4), and DI water (90−115 min, step 5).

6 Hz, which is about 2 times higher than the increase in frequency associated with the change in DNA-free solution shown in Figure 4a. This increase in frequency may be associated with either mass detachment, layer softening,[40,41] or the change in ionic strength of the electrolyte solution. For these conditions, the observed trends in frequency and dissipation variation associated with ionic strength changes of the DNA-free electrolyte solution prevent us from accurately studying plasmid adsorption reversibility.

When we doubled the plasmid concentration in the 300 mM NaCl solution to 340 mg/L, a change in the ionic strength of the rinsing solution from 300 to 30 mM NaCl resulted in almost no change in the frequency and dissipation shift (Figure 5, steps 2 and 3). However, a change of the solution from 30 to 1 mM NaCl and from 1 mM NaCl to DI water resulted in a small decrease in frequency shift and a significant increase in dissipation (Figure 5, steps 3−5). At this high concentration of plasmid DNA, the adsorbed plasmid layer is probably thick enough so that the variations in viscoelastic properties of this layer are more significant than the change due to the "buffer effect". In this case, decreases in ionic strengths of the rinsing solution from 300 to 30 mM and then to 1 mM NaCl and finally to a negligible ionic strength (i.e., DI water) do not lead to the detachment of adsorbed plasmid DNA. Interestingly, a significant increase in dissipation, when the solution was changed from 30 to 1 mM NaCl and finally to DI water, suggests that the adsorbed plasmid layer changes its conformation to a less compact and more fluid structure. This conformational change of plasmid DNA is in agreement with our observations regarding diffusion coefficients described earlier in the paper (Figure 2). Because of the relatively significant buffer effect, this set of data was not used for viscoelastic modeling in order to ensure a more quantitative assessment of the conformational changes of the adsorbed plasmid DNA layer when ionic strength is reduced. Such quantitative analysis will be presented for the QCM-D runs with divalent cations as described below.

Structure of Adsorbed Plasmid DNA in Divalent Calcium Salt Solutions. We conducted QCM-D experiments with DNA-free solutions to examine whether the buffer effect is important for adsorption runs with divalent cations. The changes in frequency and dissipation were negligible when the electrolyte solutions were changed from 1.0 mM $CaCl_2$ to 10 mM NaCl and then to 1 mM NaCl at pH 6. For example, when we switched from 1.0 mM $CaCl_2$ to 10 mM NaCl and from 10 mM NaCl to 1 mM NaCl at pH 6, we observed a change of 0.7 and 0.004 Hz in frequency over 20 min, respectively. The associated changes in dissipation were 0.05×10^{-6} and 0.06×10^{-6}. Both changes in frequency and dissipation are not higher than the inherent drift of the QCM-D baseline. Therefore, these observations allowed us to quantitatively study the reversibility of plasmid DNA adsorption, as well as the change in the structure of the adsorbed plasmid DNA layer on the silica surface in the presence of divalent cations.

Figures 6a and 7a demonstrate that after adsorption of plasmid DNA in the presence of 0.5 or 1 mM Ca^{2+}, sequential rinsing of the adsorbed plasmid DNA layer with NaCl solution at 10 mM total ionic strength and then 1 mM total ionic strength does not result in an increase in frequency shift. Thus, rinsing with calcium-free solutions and solutions with lower ionic strengths does not result in detachment of the adsorbed plasmid DNA from the silica surface. In other words, adsorption of plasmid DNA onto silica surfaces in the presence of divalent cations is irreversible, suggesting that the Ca^{2+} ion bridging between the DNA molecules and the silica surface is not removed during rinsing with Na^{+} solutions.

Cation bridging has been previously suggested in the adsorption of DNA onto sand.[13,14] Lorenz and Wackernagel[14] showed

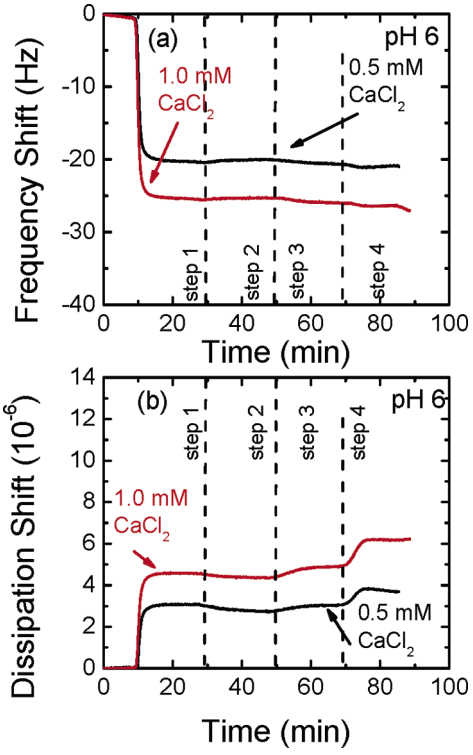

Figure 6. Frequency shift divided by the third harmonic number ($\Delta f_{(3)}$) and associated dissipation shifts ($\Delta D_{(3)}$) as a function of time for plasmid adsorption at pH 6. Plasmid DNA adsorption occurred in 10 mM total ionic strength (11−30 min, step 1) with 0.5 mM $CaCl_2$ (black line) or 1.0 mM $CaCl_2$ (red line). The adsorbed plasmid layer was washed with the corresponding $CaCl_2$ solution (30−50 min, step 2), 10 mM Na^+ solution (50−70 min, step 3), and finally with 1 mM Na^+ solution (step 4). Shown are representative data for at least two replicate measurements. Plasmid concentration was 170 mg/L and the temperature was 25 °C.

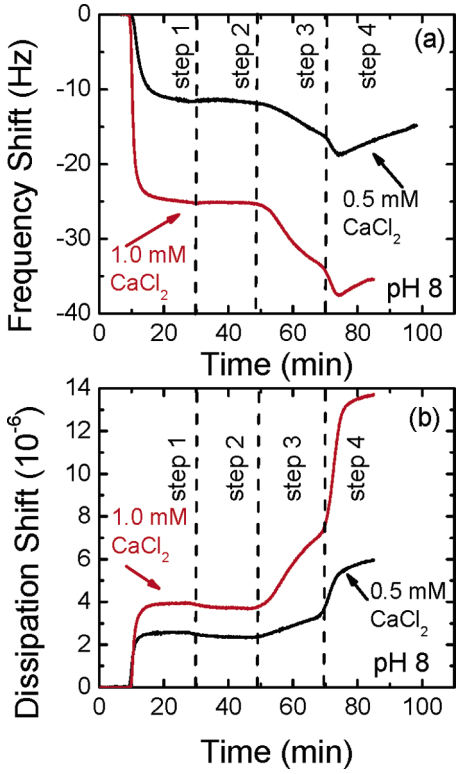

Figure 7. Frequency shift divided by the third harmonic number ($\Delta f_{(3)}$) and associated dissipation shifts ($\Delta D_{(3)}$) as a function of time for plasmid adsorption at pH 8. Plasmid adsorption occurred in 10 mM total ionic strength (11−30 min, step 1) with 0.5 mM $CaCl_2$ (black line) or 1.0 mM $CaCl_2$ (red line). The adsorbed plasmid layer was washed with the corresponding $CaCl_2$ solution (30−50 min, step 2), 10 mM Na^+ solution (50−70 min, step 3), and finally with 1 mM Na^+ solution (step 4). Shown are representative data for at least two replicate measurements. Plasmid concentration was 170 mg/L and the temperature was 25 °C.

that a substantial amount of DNA adsorbed in the presence of 200 mM $MgCl_2$ was retained in sand columns after elution with 1 M NaCl solutions. As suggested in Libera et al.[18] and Cheng et al.,[35] divalent metal cations react with the silanol groups of the silica surface via the reaction

$$-\mathrm{SiOH} + \mathrm{M}^{2+} + \mathrm{H_2O} = -\mathrm{SiOM}^{+} + \mathrm{H_3O}^{+}$$

A stability constant $\log K = -7.3$ for Ca^{2+} and silanol complexes has been reported by Stumm et al.[36] Similar to the studies of polynucleotide adsorption in Ca^{2+} solution,[18,35] the reaction of Ca^{2+} with the silanol group neutralizes negatively charged sites on the silica surface and therefore promotes adsorption of DNA molecules. The combination of specific binding of Ca^{2+} to the DNA phosphate backbone and reaction of Ca^{2+} with the silanol surface group enhances DNA adsorption to the silica surface. When the adsorbed DNA layer was exposed to 10 mM Na^+ (step 3), Na^+ can replace the Ca^{2+} cations bound solely to the DNA phosphate backbone, but not the Ca^{2+} cations bridging between silanol groups of the silica surface and the DNA phosphate backbone. Competition between monovalent and divalent cations for binding sites on the DNA phosphate backbone was proposed by Pastre et al.[21] and Cheng et al.[35]

A decrease in frequency during the rinse with 10 mM Na^+ at pH 8 (Figure 7a, step 3) is likely attributable to the uptake of water molecules by the DNA layer. The subsequent increase in frequency during the 1 mM Na^+ rinse (step 4) may be due to substantial "layer softening" as predicted previously, both theoretically[40] and experimentally.[41] For soft adsorbed layers, the resonance of the quartz crystal approaches the resonance of the adsorbed layer, giving rise to the establishment of a standing acoustic wave within the layer. In this case, much less energy is required to oscillate the layer, and therefore, the frequency increases as the layer softens.[40,41] The viscoelastic properties of the adsorbed DNA layer will be discussed in detail below.

Figures 6b and 7b demonstrate that rinsing the adsorbed layer with Na^+ solution at 10 and 1 mM total ionic strength results in an increase in dissipation, most notably at pH 8. To better illustrate the structural changes associated with variations in solution chemistry, we plot the change in dissipation ($\Delta D_{(3)}$) vs the change in the third harmonic frequency ($\Delta f_{(3)}$) as observed during the initial stage of adsorption in the presence of Ca^{2+} and during the initial stage of the subsequent rinsing. In this plot, the slopes of the lines correspond to the values of the ratios $\Delta D_{(3)}/\Delta f_{(3)}$. A small slope indicates that the adsorbed mass induces less energy dissipation, which implies that the adsorbed layer is more stiff and compact. For each experiment, linear dependences were observed during the plasmid DNA adsorption onto the silica surface and during subsequent rinsing with 10 and 1 mM Na^+ solutions. Figure 8 presents $\Delta D_{(3)}$ vs $\Delta f_{(3)}$ plots for adsorption experiments in the presence of 1.0 mM Ca^{2+} at pH 6 and 8 and for subsequent rinsing with the indicated electrolyte solutions. Data for experiments with 0.5 and 0.7 mM Ca^{2+} were not plotted but are summarized in Table 1.

For both pH 6 and 8 conditions, $\Delta D_{(3)}$ vs $\Delta f_{(3)}$ slopes are smallest in the presence of Ca^{2+}, increase during rinsing with 10 mM Na^+, and are highest during rinsing with 1 mM Na^+

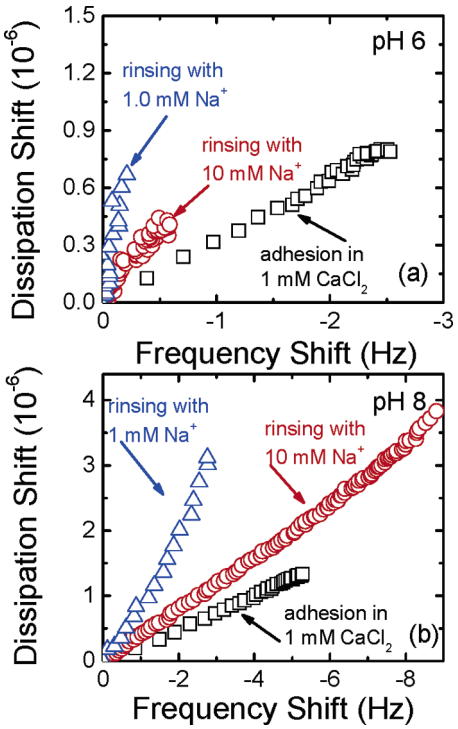

Figure 8. Dissipation shift ($\Delta D_{(3)}$) vs frequency shift ($\Delta f_{(3)}$) for plasmid adsorption at (a) pH 6 and (b) pH 8. Data for adsorption in 1 mM $CaCl_2$ were collected from 11 to 17 min, data for rinsing in 10 mM Na^+ were collected from 50 to 60 min, data for rinsing in 1 mM Na^+ were collected from 70 to 73 min, data for rinsing in 10 mM Na^+ were collected from 50 to 70 min, and data for rinsing in 1 mM Na^+ were collected from 70 to 73 min. For clarity, collected data from every 10 s were plotted. Shown are representative data for at least two replicate measurements. Plasmid concentration was 170 mg/L and the temperature was 25 °C.

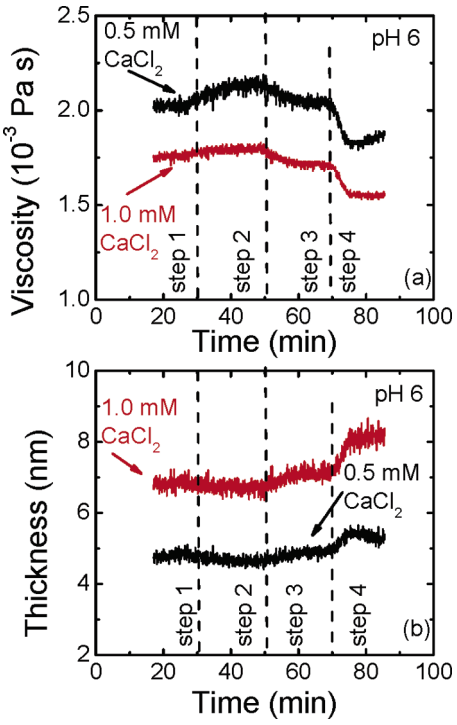

Figure 9. Plots of estimated shear viscosity and effective thickness of the adsorbed plasmid layers for different ionic compositions at pH 6. Plasmid adsorption occurred at 10 mM total ionic strength (17−30 min, step 1) with 0.5 mM $CaCl_2$ (black line) or 1.0 mM $CaCl_2$ (red line). The adsorbed plasmid layer was washed with the corresponding $CaCl_2$ solution (30−50 min, step 2), 10 mM Na^+ solution (50−70 min, step 3), and finally with 1 mM Na^+ solution (step 4). Shown are representative data for at least two replicate measurements. Plasmid concentration was 170 mg/L and the temperature was 25 °C.

(Figure 8 and Table 1). This trend suggests that the adsorbed plasmid DNA layer has a stiffer conformation in the presence of Ca^{2+} than in the presence of Na^+. When these adsorbed layers are exposed to 10 mM and then 1 mM Na^+ solutions, their structure becomes less compact or more fluid. As discussed in the context of diffusion coefficients measured by DLS, the plasmid DNA molecules have higher diffusion coefficients, and consequently, more compact conformation in the presence of Ca^{2+} than in the presence of 1 mM Na^+. Less compact conformation of plasmid DNA in 1 mM Na^+ solution leads to a less stiff adsorbed DNA layer, which dissipates more energy as the quartz crystal vibrates. Therefore, the DLS results agree quite well with the QCM-D results regarding the conformation of the plasmid DNA molecules.

To further investigate viscoelastic properties of the adsorbed DNA layer, we applied the Voigt model to calculate shear viscosity, shear modulus, and effective thickness of the adsorbed layer. This model was successfully used for DNA adsorption as previously reported.[10,25] The results are presented in Figures 9 and 10 and summarized in Table 2. Note that in some cases the Voigt-based model did not work for the first 6 min of plasmid adsorption (11−17 min), as the modeling results showed unexplainable spikes. For example, in the case of adsorption in 0.5 mM Ca^{2+} at pH 6, viscosity increased rapidly from 0.97×10^{-3} Pa s at 8.7 min to 10×10^{-3} Pa s at 9.4 min and decreased to 2.09×10^{-3} Pa s at 10.9 min and then stayed stable at around 2.03×10^{-3} Pa s. Therefore, we only report here the viscoelastic parameters obtained with the stable frequency and dissipation shift, i.e., during 17−30 min. For the first 6 min of plasmid DNA adsorption, we analyzed the data in terms of $\Delta f_{(3)}/\Delta D_{(3)}$ as presented earlier in Figure 8.

As shown in Figures 9 and 10, shear viscosity increases when the adsorbed plasmid layer is washed with Ca^{2+} solution,

Table 1. A Summary of the Slopes of Frequency Shift vs Dissipation Shift Curves for the QCM-D Experiments[a]

ionic conditions	$\Delta D_{(3)}/\Delta f_{(3)}$	ionic conditions	$\Delta D_{(3)}/\Delta f_{(3)}$
pH 6		pH 8	
adsorption in 0.5 mM Ca^{2+}	−0.27, −0.27	adsorption in 0.5 mM Ca^{2+}	−0.12, −0.24
rinsing in 10 mM Na^+	−0.55, −0.51	rinsing in 10 mM Na^+	−0.44, −0.35
rinsing in 1 mM Na^+	−1.21, −1.71	rinsing in 1 mM Na^+	−0.92, −0.93
adsorption in 0.7 mM Ca^{2+}	−0.21, −0.27	adsorption in 0.7 mM Ca^{2+}	−0.22, −0.24
rinsing in 10 mM Na^+	−0.56, −0.47	rinsing in 10 mM Na^+	−0.44, −0.39
rinsing in 1 mM Na^+	−2.47, −1.37	rinsing in 1 mM Na^+	−0.59, −0.62
adsorption in 1.0 mM Ca^{2+}	−0.33, −0.21	adsorption in 1.0 mM Ca^{2+}	−0.25, −0.24
rinsing in 10 mM Na^+	−0.78, −0.31	rinsing in 10 mM Na^+	−0.41, −0.44
rinsing in 1 mM Na^+	−2.83, −1.88	rinsing in 1 mM Na^+	−0.99, −1.13

[a] The two values in each column represent duplicate experiments. The first and second numbers in each column are the values obtained from the first and second experiment, respectively.

Table 2. Variations of Shear Viscosity, Elastic Shear Modulus, and Effective Thickness of the Adsorbed DNA Layer as a Function of Solution Ionic Composition as Calculated by the Voigt Model[a]

pH 6				pH 8			
ionic conditions	viscosity (10^{-3} Pa s)	shear modulus (10^5 Pa)	effective thickness (nm)	ionic conditions	viscosity (10^{-3} Pa s)	shear modulus (10^5 Pa)	effective thickness (nm)
adsorption in 0.5 mM Ca^{2+}	2.03, 2.00	2.01, 2.21	4.81, 4.65	adsorption in 0.5 mM Ca^{2+}	2.19, 2.16	1.84, 2.51	2.64, 4.12
rinsing in 0.5 mM Ca^{2+}	2.12, 2.06	2.12, 2.29	4.67, 4.54	rinsing in 0.5 mM $CaCl_2$	2.67, 2.29	2.51, 2.80	2.51, 4.02
rinsing in 10 mM Na^+	2.06, 1.97	2.01, 2.12	4.83, 4.75	rinsing in 10 mM Na^+	2.15, 2.12	1.94, 2.55	3.33, 4.51
rinsing in 1 mM Na^+	1.87, 1.71	1.70, 1.66	5.31, 5.50	rinsing in 1 mM Na^+	1.23, 1.61	0.74, 1.55	8.29, 6.53
adsorption in 1.0 mM Ca^{2+}	1.76, 2.30	1.50, 1.89	6.83, 4.46	adsorption in 1.0 mM Ca^{2+}	2.00, 1.97	2.33, 2.26	5.80, 5.59
Rinsing in 1.0 mM Ca^{2+}	1.79, 2.43	1.53, 2.09	6.73, 4.35	rinsing in 1.0 mM Ca^{2+}	2.06, 2.00	2.50, 2.30	5.73, 5.55
rinsing in 10 mM Na^+	1.73, 2.15	1.46, 1.51	7.03, 5.14	rinsing in 10 mM Na^+	1.79, 1.79	2.06, 1.99	7.45, 6.83
rinsing in 1 mM Na^+	1.57, 1.91	1.24, 1.35	8.00, 5.68	rinsing in 1 mM Na^+	1.36, 1.31	1.20, 1.10	12.5, 12.9

[a] The best fittings of these viscoelastic parameters are obtained using the Voigt-based model considering a single layer with a fixed density of 1030 kg/m^3 in all cases. Shown values are the average of all values collected as follows: plasmid adsorption (17−30 min), rinse in Ca^{2+} (30−50 min), rinse in 10 mM Na^+ (50−70 min), and rinse in 1 mM Na^+ (70−85 min). The two values in each column represent duplicate experiments. The first and second numbers in each column are the values obtained from the first and second experiment, respectively.

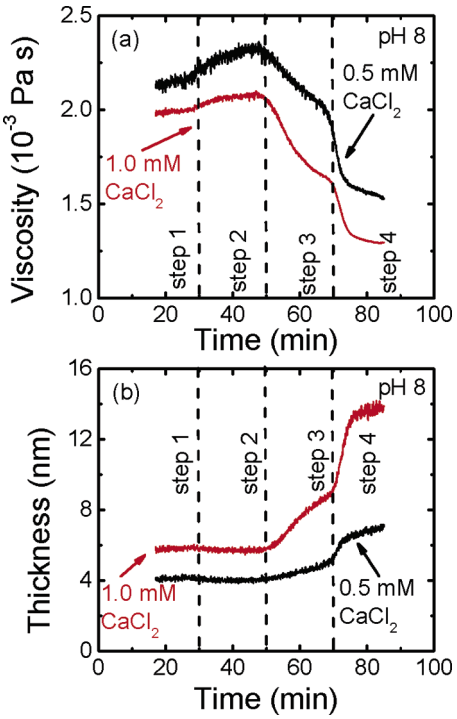

Figure 10. Plots of estimated shear viscosity and effective thickness of the adsorbed plasmid layers for different ionic compositions at pH 8. Plasmid adsorption occurred at 10 mM total ionic strength (17−30 min, step 1) with 0.5 mM $CaCl_2$ (black line) or 1.0 mM $CaCl_2$ (red line). The adsorbed plasmid layer was washed with the corresponding $CaCl_2$ solution (30−50 min, step 2), 10 mM Na^+ solution (50−70 min, step 3), and finally with 1 mM Na^+ solution (step 4). Shown are representative data for at least two replicate measurements. Plasmid concentration was 170 mg/L and the temperature was 25 °C.

gradually decreases during the wash with 10 mM Na^+ solution, and becomes lowest when washed with 1 mM Na^+ solution. The calculated shear modulus also showed a similar trend as the calculated viscosity (Table 2). This trend in the calculated shear viscosity and shear modulus suggests that, in a Ca^{2+} solution, the adsorbed plasmid layer is stiff and becomes softer and more "liquid-like" in a Na^+ solution. In addition, the calculated effective thickness is smallest in the presence of Ca^{2+}, increases in the presence of 10 mM Na^+, and becomes highest in the presence of 1 mM Na^+. This increase in the adsorbed layer thickness indicates that rinsing the adsorbed layer with a Na^+ solution leads to a softer layer with a less compact DNA conformation and more incorporated water molecules. Experimental studies on solvated Mg^{2+} and Ca^{2+} ions binding to DNA molecules via hydrogen bond have been reported in the literature.[32,33,42,43] Similar to solvated divalent cations in water, DNA molecules are hydrated and surrounded by hydration shells. Interactions between the divalent cations and the DNA molecules are accompanied by the overlapping of their hydration shells. As a result, water molecules are released upon Ca^{2+} binding to the DNA molecules. In addition, Subirana and Soler-Lopez[42] reviewed studies suggesting that Mg^{2+} and Ca^{2+} can be replaced by other ions or water molecules.

Compared to pH 6, the changes in frequency, dissipation, viscosity, shear modulus, and effective thickness of the adsorbed layer at pH 8 are more pronounced (Table 2). For example, switching from 1 mM Ca^{2+} to 10 mM Na^+ results in a decrease in viscosity by 0.1×10^{-3} and 0.4×10^{-3} Pa s for pH 6 and 8, respectively. This difference in viscosity shift is related to the fact that $f_{(3)}$ decreases by 0.5 and 8.0 Hz, and $D_{(3)}$ increases by 0.4×10^{-6} and 4.0×10^{-6}, respectively (Figures 6−8). A higher decrease in frequency and a higher increase in dissipation at pH 8 indicate a softer DNA layer. Specifically, during rinsing of the plasmid DNA adsorbed layer with 1 mM Na^+, shear viscosities of the adsorbed layers are higher at pH 6 than at pH 8 (Table 2). The effective thickness of the DNA layer at pH 6 is lower than at pH 8 (Table 2). In our case, it is possible that the adsorbed supercoiled plasmid DNA molecules are more flexible at pH 6 than at pH 8 because there are more OH^- groups surrounding the DNA molecules at pH 8. Consequently, upon changing Ca^{2+} concentrations, more water molecules are incorporated in the DNA adsorbed layer at pH 8 than at pH 6, resulting in a decrease in frequency (step 3, Figure 7a), and a higher change in viscosity, shear modulus, and effective thickness of the adsorbed layer.

Conclusion

The QCM-D results suggest that electrostatic interactions control plasmid DNA adsorption onto silica surfaces. Two kinds of electrostatic interactions need to be considered: (1) interactions between the plasmid DNA molecules and silica surface and (2) interactions among subunits of the plasmid DNA molecules that control plasmid DNA conformation. In low ionic strength solutions containing 1.0 mM Ca^{2+}, plasmid DNA adsorption to silica is fast and irreversible. For monovalent salt at the highest ionic strength examined (300 mM NaCl), the adsorption rate is merely 1% of that under nonrepulsive

(favorable) conditions (attachment efficiencies of 0.03 and 0.01 at pH 6 and 8, respectively). Charge neutralization upon Ca^{2+} binding to the DNA phosphate groups increases the adsorption rate dramatically, resulting in attachment efficiencies near unity (0.75 and 0.87 with 1 mM Ca^{2+} at pH 6 and 8, respectively). The absence of detachment of plasmid DNA molecules from the silica surface when the adsorbed layer is rinsed with 10 or 1 mM Na^{+} solutions may indicate bridging by specific binding of Ca^{2+} to both the phosphate backbones and the silica surface.

The combined results from QCM-D and DLS experiments suggest that DNA molecules and the DNA adsorbed layer have a compact and stiff conformation in the presence of 1 mM Ca^{2+}. However, in solutions containing 10 or 1 mM Na^{+}, the adsorbed layer is more fluid and has a much less stiff conformation. When the adsorbed DNA layer formed in the presence of Ca^{2+} is exposed to Na^{+} solutions at equal and lower ionic strengths, the DNA layer relaxes to a less compact and rigid conformation.

Acknowledgment. Funding was provided by the Yale Institute for Biospheric Studies and the National Science Foundation (BES 0228911). We would like to thank Dr. Paul Van Tassel for letting us use the QCM-D, Dr. Barbara Kazmierczak for providing the bacterial strain, and Kai Loon Chen for the DLS experiments.

References and Notes

(1) Pease, A. C.; Solas, D.; Sullivan, E. J.; Cronin, M. T.; Holmes, C. P.; Fodor, S. P. A. *Proc. Natl. Acad. Sci. U.S.A.* **1994**, *91*, 5022−5026.
(2) Schena, M.; Shalon, D.; Heller, R.; Chai, A.; Brown, P. O.; Davis, R. W. *Proc. Natl. Acad. Sci. U.S.A.* **1996**, *93*, 10614−10619.
(3) Cheng, L.; Ziegelhoffer, P. R.; Yang, N. S. *Proc. Natl. Acad. Sci. U.S.A.* **1993**, *90*, 4455−4459.
(4) Radler, J. O.; Koltover, I.; Salditt, T.; Safinya, C. R. *Science* **1997**, *275*, 810−814.
(5) Mannelli, F.; Minunni, A.; Tombelli, S.; Wang, R. H.; Spiriti, M. M.; Mascini, M. *Bioelectrochemistry* **2005**, *66*, 129−138.
(6) Pedano, M. L.; Rivas, G. A. *Biosens. Bioelectron.* **2003**, *18*, 269−277.
(7) Pedano, M. L.; Rivas, G. A. *Sensors* **2005**, *5*, 424−447.
(8) Ferreira, G. N. M. *Chem. Eng. Technol.* **2005**, *28*, 1285−1294.
(9) Hook, F.; Ray, A.; Norden, B.; Kasemo, B. *Langmuir* **2001**, *17*, 8305−8312.
(10) Larsson, C.; Rodahl, M.; Hook, F. *Anal. Chem.* **2003**, *75*, 5080−5087.
(11) Hansma, H. G.; Laney, D. E.; Bezanilla, M.; Sinsheimer, R. L.; Hansma, P. K. *Biophys. J.* **1995**, *68*, 1672−1677.
(12) Branda, S. S.; Vik, A.; Friedman, L.; Kolter, R. *Trends Microbiol.* **2005**, *13*, 20−26.
(13) Romanowski, G.; Lorenz, M. G.; Wackernagel, W. *Appl. Environ. Microbiol.* **1991**, *57*, 1057−1061.
(14) Lorenz, M. G.; Wackernagel, W. *Appl. Environ. Microbiol.* **1987**, *53*, 2948−2952.
(15) Maier, B.; Chen, I.; Dubnau, D.; Sheetz, M. P. *Nat. Struct. Biol.* **2004**, *11*, 643−649.
(16) Lorenz, M. G.; Wackernagel, W. *Microbiol. Rev.* **1994**, *58*, 563−602.
(17) Poly, F.; Chenu, C.; Simonet, P.; Rouiller, J.; Monrozier, L. J. *Langmuir* **2000**, *16*, 1233−1238.
(18) Libera, J. A.; Cheng, H.; de la Cruz, M. O.; Bedzyk, M. J. *J. Phys. Chem. B* **2005**, *109*, 23001−23007.
(19) Bezanilla, M.; Manne, S.; Laney, D. E.; Lyubchenko, Y. L.; Hansma, H. G. *Langmuir* **1995**, *11*, 655−659.
(20) Hansma, H. G.; Laney, D. E. *Biophys. J.* **1996**, *70*, 1933−1939.
(21) Pastre, D.; Pietrement, O.; Fusil, P.; Landousy, F.; Jeusset, J.; David, M. O.; Hamon, C.; Le Cam, E.; Zozime, A. *Biophys. J.* **2003**, *85*, 2507−2518.
(22) Pietrement, O.; Pastre, D.; Fusil, S.; Jeusset, J.; David, M. O.; Landousy, F.; Hamon, L.; Zozime, A.; Le Cam, E. *Langmuir* **2003**, *19*, 2536−2539.
(23) Voinova, M. V.; Rodahl, M.; Jonson, M.; Kasemo, B. *Phys. Scr.* **1999**, *59*, 391−396.
(24) Gurdak, E.; Dupont-Gillain, C. C.; Booth, J.; Roberts, C. J.; Rouxhet, P. G. *Langmuir* **2005**, *21*, 10684−10692.
(25) Stengel, G.; Hook, F.; Knoll, W. *Anal. Chem.* **2005**, *77*, 3709−3714.
(26) Wilfinger, W. W.; Mackey, K.; Chomczynski, P. *BioTechniques* **1997**, *22*, 474−&.
(27) Manchester, K. L. *BioTechniques* **1995**, *19*, 208−210.
(28) Liu, H.; Gapinski, J.; Skibinska, L.; Patkowski, A.; Pecora, R. *J. Chem. Phys.* **2000**, *113*, 6001−6010.
(29) Seils, J. C.; Pecora, R. *Macromolecules* **1992**, *25*, 354−362.
(30) Hammermann, M.; Brun, N.; Klenin, K. V.; May, R.; Toth, K.; Langowski, J. *Biophys. J.* **1998**, *75*, 3057−3063.
(31) Newman, J.; Tracy, J.; Pecora, R. *Macromolecules* **1994**, *27*, 6808−6811.
(32) Minasov, G.; Tereshko, V.; Egli, M. *J. Mol. Biol.* **1999**, *291*, 83−99.
(33) Kankia, B. I. *Biophys. Chem.* **2000**, *84*, 227−237.
(34) Stuart, M. A. C.; Hoogendam, C. W.; deKeizer, A. *J. Phys.: Condens. Matter* **1997**, *9*, 7767−7783.
(35) Cheng, H.; Zhang, K.; Libera, J. A.; de la Cruz, M. O.; Bedzyk, M. J. *Biophys. J.* **2006**, *90*, 1164−1174.
(36) Stumm, W.; Hohl, H.; Dalang, F. *Croat. Chem. Acta* **1976**, *48*, 491−504.
(37) Ellis, J. S.; Abdelhady, H. G.; Allen, S.; Davies, M. C.; Roberts, C. J.; Tendler, S. J. B.; Williams, P. M. *J. Microsc.*—Oxford **2004**, *215*, 297−301.
(38) Stockbridge, C. D. *Vacuum Microbalance Techniques*; Plenum: New York, 1966; Vol. 5.
(39) Goubaidoulline, C.; Reuber, J.; Merz, F.; Johannsmann, D. *J. Appl. Phys.* **2005**, *98*.
(40) Lucklum, R.; Behling, C.; Hauptmann, P. *Anal. Chem.* **1999**, *71*, 2488−2496.
(41) Graneli, A.; Edvardsson, M.; Hook, F. *Chemphyschem* **2004**, *5*, 729−733.
(42) Subirana, J. A.; Soler-Lopez, M. *Annu. Rev. Biophys. Biomol. Struct.* **2003**, *32*, 27−45.
(43) Kankia, B. I.; Marky, L. A. *J. Phys. Chem. B* **1999**, *103*, 8759−8767.

BM0603948